Design and Development of a 66-W/kg, 23-m² Roll-Up Solar Array

W. A. Hasbach

Guidance and Control Division

Future space missions will require greater power output, lighter weight, and decreased stowed volume for solar arrays. To meet these requirements, a program was initiated to develop the technology for a roll-up solar array by preparing a detailed design, performing the associated analyses, fabricating an engineering development model, and subjecting the engineering model to a comprehensive test program consisting of both environmental and developmental tests. The design and testing of the 66-W/kg (30-W/lb),[1] 23-m² (250 ft²) roll-up solar array developed during this program is described in this article.

Introduction

Future space missions will require greater power output, lighter weight, and decreased stowed volume for solar arrays. To meet these requirements, a program was initiated to develop the technology for a roll-up solar array by preparing a detailed design, performing the associated analyses, fabricating an engineering development model, and subjecting the engineering model to a comprehensive test program consisting of both environmental and developmental tests. The design chosen is adaptable to a variety of vehicle configurations and missions, including solar electric propulsion for unmanned planetary exploration and the manned space station for Earth orbiters.

Description

The design of the array was based upon the results of an earlier feasibility study by the General Electric Company (Reference 1). With this

[1]Where applicable, the International System of Units is stated first, followed by the customary units in parentheses. In each case, the value in parentheses represents the measured or calculated unit.

design, a 23-m^2 solar cell module area would be stored on drums until deployment of the array after launch. The array, in its fully deployed configuration, is illustrated in Figure 1. The dimensions of each panel are 1.17 m (46 in.) × 10.21 m (402 in.).

The engineering test model is representative of a flight-type design, except for a limited solar cell coverage; 4000 solar cells were bonded to the substrates, with the remaining area occupied by glass platelets to simulate the solar cell mass and interconnect bending stiffness. The locations of the various components on the engineering test model are shown in Figure 2. The weight breakdown for the model is as follows:

Component	Weight, kg
Array substrate assemblies	10.532 10.596
Solar panel actuator	5.321
Storage drum assemblies (2)	7.983
Drum-to-center-support mounting hardware	0.059
Center support	0.603
Leading edge member	0.386
Leading-edge-member support brackets (2)	0.099
Outboard end supports (2)	1.860
Total	37.439

Based on the above weights, the array power-to-weight ratio is 67 W/kg. This ratio is based on the ability of the array to generate 2500 W of power at 328 K (55°C) under "air mass zero" illumination and within ±0.1745-rad orientation with the Sun at 1.49599 × 10^8 km (1.0 AU), compared to a power-to-weight ratio of approximately 22 W/kg for typical *Mariner*-type solar panels. Cell efficiency is specified by area performance of 107.6 W/m^2 (10 W/ft^2) of gross module area. The cell selected to achieve minimum weight was 0.020 cm thick, 2 cm × 2 cm, with 3.8 cm^2 of active area per cell. The calculated array power under these conditions is 2523 W at 102 Vdc. To arrive at the maximum power available at the electrical interface on the center support, the series resistance distribution losses in the array substrate bus strip, the slip ring (including line losses within the storage drum and center support), and the solar cell interconnect were taken into account. The effect of the combined series resistance loss is to reduce the maximum power by 57 W at an operating temperature of 328 K.

The major components that form the power-producing system are described below.

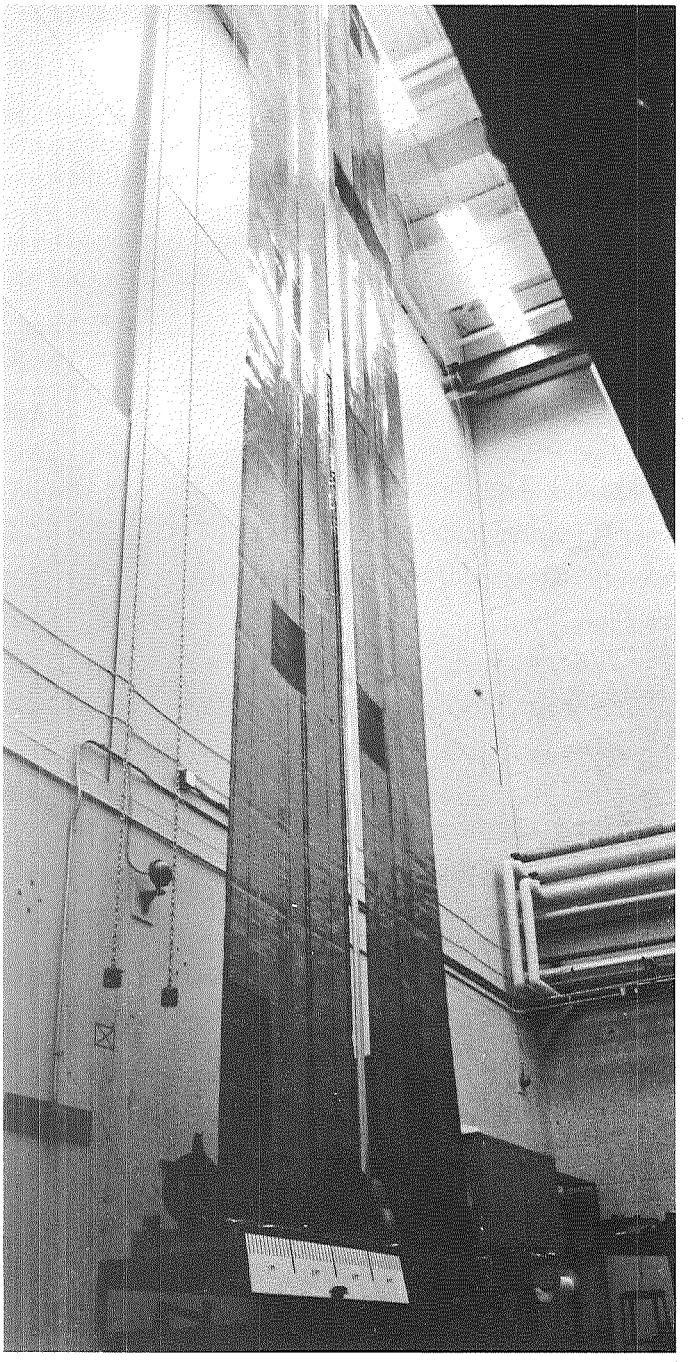

Figure 1. Fully deployed solar array

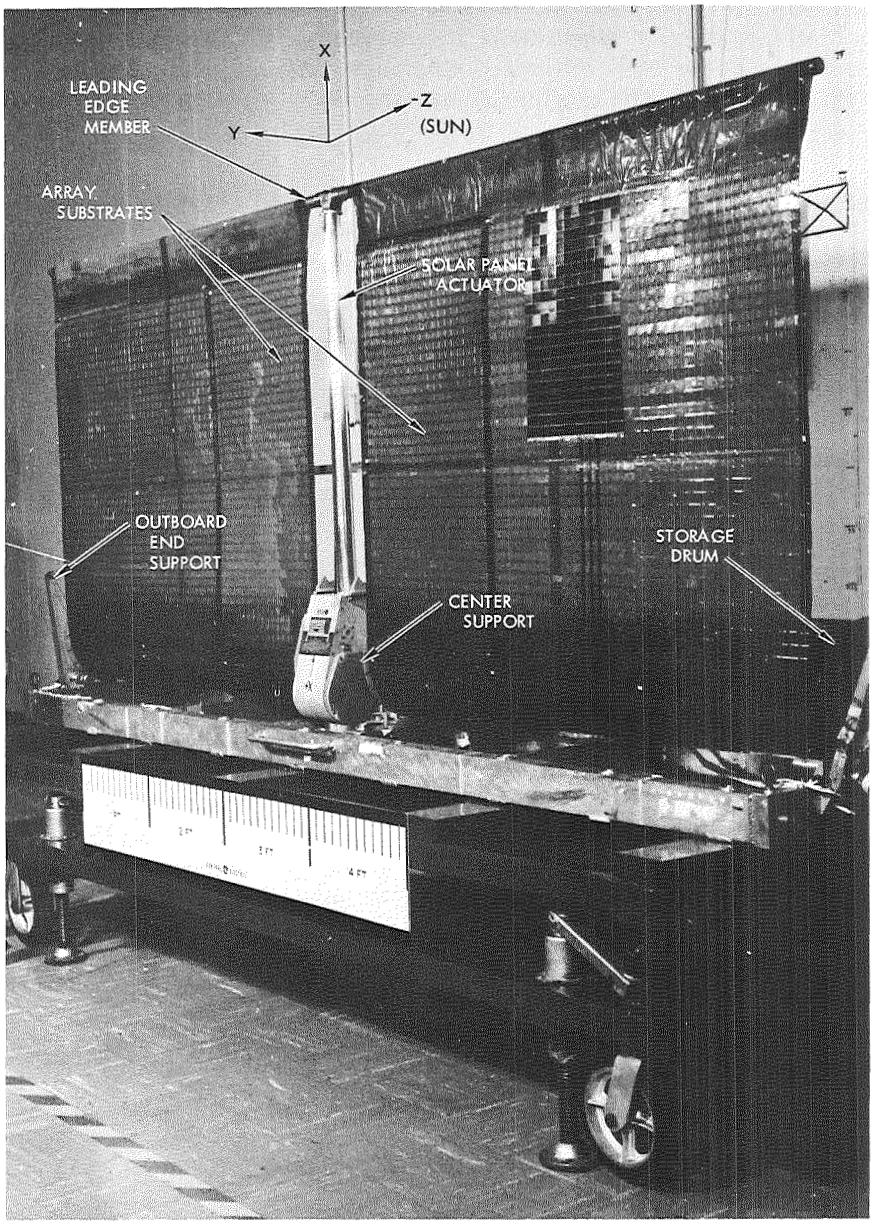

Figure 2. Solar array components

Array Substrate

The solar cells are mounted on two flexible substrates of 0.005-cm Kapton H film. Tension in these two substrates is utilized to maintain the desired single-plane geometry and to establish the natural frequency of the deployed system above the required 0.04 Hz. The flight-type design calls for each substrate to support 6 circuits, each composed of 12 series-connected modules (eleven with 20 series cells by 19 parallel cells and one with 22 series cells by 19 parallel cells).

The substrate is fabricated from copper-clad Schjel-Clad L-7510 etched to form a conductor electrical bus strip system, with each circuit feeding into the main positive and negative bus. The bus in turn connects to the feed-through section of the drum and the slip rings. All connections from the cell side of the substrate to the bus strip system are made around the edges rather than through holes in the substrate. The exposed copper bus strips on the rear side of the substrate are covered with Kapton silicone pressure-sensitive tape. Foamed RTV 560 cushioning buttons are deposited on the rear side of the substrate at the corners of each solar cell. These buttons provide the required interlayer cushioning in the stowed configuration.

Solar Panel Actuator

The solar panel actuator is a Bi-Stem deployable boom unit designed and developed by Spar Aerospace Products, Ltd. The boom element, the component which provides the actuation force for deployment and forms the primary structure in the deployed configuration, has a nominal outside diameter of 3.4 cm (1.34 in.). It is made up to two 301 stainless-steel strips, 10.2 cm (4 in.) wide and 0.018 cm (0.007 in.) thick, which are prestressed to form an overlapped tube in the deployed position. The boom is silver-plated on its outside surfaces to reduce the temperature gradients in the boom when one side is exposed to solar radiation and the other side is in shadow.

Storage Drums

The two storage drums in the system form the backbone of the stowed configuration. The drums rotate approximately 15 turns to deploy or retract the array. Each drum includes a shell, outboard end cap, inboard end cap, and edge guides. The drum shells are 1.196-m (47.10 in.)-long, 0.081-cm (0.032 in.)-thick sheet magnesium rolled into a 20.32-cm (8-in.)-diameter cylinder, which is closed with a lap-butt joint utilizing 1.9-cm (0.75 in.)-wide strip of magnesium bonded with Epon 934.

The inboard end cap assembly houses the two main bearings which allow the storage drum to rotate with respect to the support shaft. The constant torque negator spring motor, which provides the substrate preload force, is mounted on the inboard end cap with the output spool

coaxial with the main bearings. A slip ring assembly, which functions to transfer array power and signals across the rotary joint between the drums and the center support, is then mounted to the inboard end of this output spool. The outboard end cap serves as the supporting interface for the drum outer end during launch. It contains a tapered hole which mates with a tapered plug in the outboard end support. Two edge guide flanges are mounted on each storage drum to provide control forces to the substrate edge if required during retraction.

Center Support

The center support consists of a magnesium center tube, two machined magnesium end fittings, and two magnesium face sheets. The center tube is pinned to the end fittings, and the face sheets are riveted to the tube end fittings. One face sheet provides for the electrical connector installation and, together with the other face sheet, transmits shear loads. The end fittings provide the interface pads for the vehicle structure and the solar panel actuator.

Leading Edge Member

The leading edge member is the structural element on the outer-most edge of the substrate. In the deployed configuration, this member transmits the 17.8-N (4-lb) substrate preload force from the array substrates to the boom tip. In the stowed configuration, the leading edge member functions to restrain the outer substrate wrap and to cage the Bi-Stem boom element. The tips of this member are supported by the outboard end supports, and the center section is supported from the actuator housing by two saddle-type brackets. The leading edge member is made up from two 1.27-m (50.1-in.)-long cylinders fabricated from 0.05-cm (0.020 in.) beryllium sheet bonded with Epon 934. The two cylinders are inserted into a center fitting and bonded in place. This fitting also houses two instrument bearings which mate with the stainless-steel boom post. These bearings decouple the array substrate from the Bi-Stem boom for rotation about the boom axis.

Outboard End Support

This arm carries the stainless-steel tapered plugs which interface with the outboard end cap and leading edge member. Attachment of the movable arm to the vehicle-mounted bracket is through a hinge joint. A torsion spring which mounts on the hinge pin furnishes 1130 N-cm (100 in.-lb) of torque in the stowed configuration. The release of the support is accomplished by a separation nut/separation bolt/bolt catcher combination. The torsion spring forces the movable arm to rotate about the hinge pin through an angle of approximately 0.17 rad. The storage drum and the leading edge member are thus released to permit deployment of the solar panel actuator.

Testing

The engineering test model was subjected to a comprehensive test program consisting of both environmental and developmental tests. The following tests were conducted:

(1) Deployed dynamics tests to provide necessary data on the dynamic characteristics of the deployed array for use in a comparison with analytical data. Results of the comparison were used to verify the mathematical models generated in earlier phases of the program or to provide information to improve the mathematical models. During the tests, the array was deployed vertically downward in a vacuum chamber, and the system was excited with motion at the center support. Out-of-plane symmetric (Z-axis), out-of-plane antisymmetric (torsional), and in-plane (Y-axis) excitations were performed.

(2) Pyrotechnic-induced shock tests to measure acceleration levels on the array components resulting from the simultaneous firing of both separation nuts (each armed with two active squibs) on the outboard end supports.

(3) Thermal–vacuum tests to measure response of the array under deployed transient, low-temperature stowed, low-temperature deploy and retract, stowed transient and high-temperature soak, and high-temperature deploy and retract conditions.

(4) Acoustic noise test to monitor response of system exposed to 60 s of random incidence, reverberent sound with an overall sound pressure level of 150 dB.

(5) Stowed vibration tests in Y-, Z-, and X-axes. The tests consisted of: (a) several low-level sinusoidal sweeps to set initial recording gain factors and to obtain array response to a constant-level base excitation input to determine amplification factors, (b) an acceptance-level sinusoidal sweep at two-thirds of the specification level to evaluate linearity of system response and to provide a final assessment of the risks associated with the full-level qualification input, (c) a sinusoidal qualification sweep, and (d) random noise testing with the same sequence (low-level, acceptance-level, and qualification-level testing).

Test Performance

Cell/Coverglass/Glass Platelet Breakage

The percent of solar cell and coverglass breakage resulting from the environmental test program was significantly greater than that for

the dummy glass platelets. Breakage followed the relative difference in individual element thickness, i.e.,

Item	Total breakage, %
0.007-cm coverglass	3.25
0.020-cm solar cells	1.75
0.028-cm dummy glass platelets	0.47

The most severe environment for the coverglass and solar cells was the stowed vibration test. There is no breakage pattern to indicate a possible cause for the high proportion of damage in the case of the coverglass, although there are a few examples of parallel adjacent coverglass as within a module row that have cracked in a direction parallel to the axis of the storage drum. This may be an indication of insufficient cushioning between the storage drum shell and the first wrap of solar cells.

The results indicate that the cell/coverglass composite is not as resistant to damage as a corresponding glass platelet mass simulation that is 0.028 cm thick. The 0.007-cm-thick coverglass cracked independently of the cell in many cases. Since some of the damage was sustained during the acoustic noise test, it is felt that a test of this type should be retained as a system test environment for future lightweight solar array assemblies.

The thermal–vacuum tests represented the most severe environment for the dummy glass platelets. This may be explained by the fact that the areas of dummy glass were not temperature-controlled during the deploy and retract cycles and therefore were colder than the solar cell modules. Also, many localized areas of the dummy glass were affected by an overheating condition that occurred during the stowed high-temperature test. Either of these factors could account for the disproportionate percentage of glass platelet breakage during these tests.

Solar Panel Actuator Limit Switch Failures

Three microswitches are required within the solar panel actuator to maintain the fully retracted, orbital retracted (10.16 cm from fully retracted), and fully extended positions. At the conclusion of testing, none of these switches were operable. Since their function was not vital, no effort was made to fix the switches. The redesign required for corrective action is considered minimum for future applications.

Fatigue Cracking Near Leading Edge Member

A fatigue crack 0.317 cm (⅛ in.) long, near the leading edge member in the solar panel actuator rod outer element, was discovered while pre-

paring for a 35-cycle life demonstration following the stowed vibration test. No change in performance of the system or in the length of the crack was detected during or after the life demonstration.

Slip Ring Resistance Changes

At the beginning of the test program, the slip ring resistance remained constant as the storage drums turned during array deployment and retraction. Some slip ring dynamic resistance change was first recorded during the low-temperature deploy and retract cycle. Similar fluctuations, along with a slight overall increase in resistance, were recorded during the high-temperature deploy and retract cycle. The first ambient deployment following the stowed vibration test produced fluctuations in resistance which corresponded to the period of rotation of the storage drums. After 35 ambient deploy and retract cycles, the magnitude of these fluctuations in resistance had decreased. The periodic nature of the changes in resistance indicates the possibility of dirt on the power rings which was gradually removed by the brushes as the array was deployed and retracted during the 35-cycle life demonstration. There was no significant increase in the static resistance of the power rings as a result of the environmental test program.

Marginal Performance of Storage Drum Negator Spring System

The present storage drum negator spring system appeared marginal for rewrap of the array substrate during the low-temperature deploy and retract test.

Reliability Demonstration

At the conclusion of the total test program, the array was deployed to its full length and retracted 35 additional times to establish confidence in such items as cell interconnects, deployment/retraction components, and slip ring assemblies. In all, more than 100 deployment retraction cycles were performed during the term of this program. With the exception of the microswitch failures noted above, no anomalies were detected which could be attributed to rolling and unrolling the solar cell substrates on the storage drums. During the performance of the deployment/retraction tests, the deployment boom was purposely offset from its center line in the plane of the substrate to determine the array's ability to rewrap uniformly. It was demonstrated in these experiments that a boom tip deflection of up to 21 cm can be accommodated without difficulty and uniform substrate wrapping will not be compromised.

Conclusion

Since the array demonstrated its ability to survive the specified test program, the concept of this 23-m^2 roll-up solar array with a 66-W/kg power-to-weight ratio has been proven feasible.

Reference

1. *Feasibility Study 30 Watts Per Pound Roll Up Solar Array Final Report,* Report 68SD4301. General Electric Co., Philadelphia, Pa., June 21, 1968.